Journal of Cerebral Blood Flow & Metabolism (2011) 31, 293–304

www.jcbfm.com

Characterization of *in vivo* pharmacokinetic properties of the dopamine D1 receptor agonist DAR-0100A in nonhuman primates using PET with [^{11}C] NNC112 and [^{11}C] raclopride

Mark Slifstein[1,2], Raymond F Suckow[2], Jonathan A Javitch[1,2,3], Thomas Cooper[2], Jeffrey Lieberman[1,2] and Anissa Abi-Dargham[1,2,4]

[1]*Department of Psychiatry, Columbia University, New York, New York, USA;* [2]*New York State Psychiatric Institute, New York, New York, USA;* [3]*Department of Pharmacology, Columbia University, New York, New York, USA;* [4]*Department of Radiology, Columbia University, New York, New York, USA*

DAR-0100A, the active enantiomer of dihydrexidine, is a potent dopamine D1 agonist under investigation for treatment of cognitive impairment and negative symptoms of schizophrenia. We measured the dose–occupancy relationship for DAR-0100A at D1 receptors using positron emission tomography (PET) imaging in baboons with [^{11}C] NNC112 and its binding to D2 with [^{11}C] raclopride. Two baboons were scanned with [^{11}C] NNC112 at baseline and after three different doses of DAR-0100A. Two baboons were scanned with [^{11}C] raclopride at baseline and after one dose of DAR-0100A. Occupancy (ΔBP_{ND}) was computed in the striatum and cortex. A clear relationship was observed between plasma concentration of DAR-0100A and ΔBP_{ND}. ΔBP_{ND} was larger in the striatum than in the cortex, consistent with reports showing that 25% of [^{11}C] NNC112 BP_{ND} in the cortex is attributed to 5-HT_{2A}. Plasma EC_{50} estimates ranged from 150 to 550 ng/mL according to the constraints on the model. There was no detectable effect of DAR-0100A on [^{11}C] raclopride BP_{ND}. These data suggest that at doses likely to be administered to patients, occupancy will not be detectable with [^{11}C] NNC112 PET and binding of DAR-0100A to D2 will be negligible. This is the first demonstration with PET of a significant occupancy by a full D1 agonist *in vivo*.
Journal of Cerebral Blood Flow & Metabolism (2011) **31,** 293–304; doi:10.1038/jcbfm.2010.91; published online 23 June 2010

Keywords: [^{11}C] NNC112; DAR-0100A; dopamine D1 receptors; D1 agonist; PET; positron emission tomography

Introduction

A large number of effective pharmacological interventions have been introduced over the past five decades for the treatment of the positive symptoms of schizophrenia, but efforts to treat the cognitive and negative symptoms have been less successful. Several lines of research in preclinical species and in laboratory preparations have led to the suggestion that dopamine D1 receptor agonists may improve working memory in patients with schizophrenia, a function performed poorly by many patients (Aleman *et al*, 1999). For example, Goldman-Rakic *et al* (2004) assembled an extensive body of work showing the importance of adequate prefrontal cortical D1 receptor stimulation for optimal performance of spatial working memory tasks by nonhuman primates. Studies have shown working memory improvement by administration of D1 agonists in primate models of cortical dopaminergic hypofunction (Arnsten *et al*, 1994; Schneider *et al*, 1994; Castner *et al*, 2000). Seamans and colleagues have suggested a model of cortical working memory in which there are D1 and D2 dominated states, with the D1 state having an essential role in optimal working memory function (Seamans *et al*, 2001; Durstewitz and Seamans, 2002, 2008; Seamans and Yang, 2004; Trantham-Davidson *et al*, 2004). Patients with schizophrenia have been hypothesized to have low dopamine function in the prefrontal cortex, and thus there is considerable interest in exploring the potential of D1 agonists as cognitive enhancers in schizophrenia.

DAR-0100 (dihydrexidine) is a potent D1 agonist (Mottola *et al*, 1992). The safety of acute doses has been shown in patients with schizophrenia (George *et al*, 2007). DAR-0100A is the active (+) enantiomer

Correspondence: Dr M Slifstein, Department of Psychiatry, New York State Psychiatric Institute, Unit 31, 1051 Riverside Drive, New York, NY 10032, USA.
E-mail: mms218@columbia.edu
This study was supported by NIMH U01 MH076544.
Received 30 March 2010; revised 20 May 2010; accepted 2 June 2010; published online 23 June 2010

of the racemic mixture DAR-0100 (Knoerzer *et al*, 1994). *In vitro*, DAR-0100A has 125-fold higher affinity for D1 receptors than the (−) enantiomer, and in functional assays (stimulated adenylate cyclase activity), virtually all activities are attributable to the (+) enantiomer, with maximal activity comparable with that of dopamine (Knoerzer *et al*, 1994). Thus, there is interest in testing DAR-0100A as a therapy for cognitive deficits in schizophrenia, but the doses to be administered are not easily identifiable. DAR-0100A also has ~16-fold lower *in vitro* affinity for dopamine D2 receptors than for D1 receptors (Knoerzer *et al*, 1994) and displays an agonist-like property (inhibition of prolactin release) at D2 receptors (Mottola *et al*, 1992). At present, very little is known about the *in vivo* pharmacokinetic properties of DAR-0100A. The goal of this study was to use positron emission tomography (PET) imaging in baboons to characterize its *in vivo* pharmacokinetic properties at D1 and D2 receptors, using [^{11}C] NNC112 and [^{11}C] raclopride for probes at D1 and D2, respectively. We administered DAR-0100A by intravenous infusion to anesthetized baboons over a range of concentrations up to 9 mg/kg, which is approximately a 60-fold greater concentration of the active enantiomer than contained in the 20 mg of racemic DAR-0100 administered to human subjects in the study by George *et al* (2007), and compared [^{11}C] NNC112 binding during drug administration with baseline values to establish a dose–occupancy relationship. We also scanned baboons before and after large doses of DAR-0100A with [^{11}C] raclopride to determine whether binding to D2 receptors was detectable.

There are two PET radioligands in the widespread use for imaging D1 receptors: [^{11}C] NNC112 and [^{11}C] SCH 23390. We have shown that ~25% to 30% of the specific binding in the cortex of anesthetized baboons of both of these ligands is attributable to 5-HT$_{2A}$ receptors, whereas virtually all detectable specific binding in the striatum is attributed to D1 (Ekelund *et al*, 2007). We have also shown that a similar binding profile occurs for [^{11}C] NNC112 in awake human subjects (Slifstein *et al*, 2007). As DAR-0100A has negligible affinity for 5-HT$_{2A}$, we predicted that 20% to 30% of specific binding by [^{11}C] NNC112 in the cortex would be inaccessible to competition from DAR-0100A, so that the percentage decrease in binding observed in the cortex during DAR-0100A administration compared with baseline would be less than that in the striatum by this factor.

Materials and methods

Subjects

Three adult male baboons (baboons A, B, and C, *Papio anubis*, weighing 20.4 ± 4.3 kg) were scanned in this study. Baboons were scanned with [^{11}C] NNC112 at baseline and following 1.5, 3, and 6 mg/kg of DAR-0100A (A), or 1.5, 3, and 9 mg/kg of DAR-0100A (B). Baboon A was also scanned with [^{11}C] raclopride at baseline and following 5 mg/kg on two different occasions; baboon C was scanned with [^{11}C] raclopride at baseline and following 3 mg/kg DAR-0100A. The study procedures were approved by the IACUC (Institutional Animal Care and Use Committees) of the Columbia University and New York State Psychiatric Institute.

DAR-0100A Preparation and Administration

In each experiment, DAR-0100A was dissolved in 60 mL of saline vehicle. DAR-0100A was administered as a constant intravenous infusion starting 10 minutes before the start of the drug condition scan. The solution was delivered using a programmable syringe pump (Harvard Apparatus, Holliston, MA, USA). The infusion rate was set such that delivery of the entire 60 mL volume coincided with the duration of the scan, i.e., the rate was 60 mL/(scan duration + 10 minutes).

Radiochemistry

[^{11}C] NNC112 was prepared as described in the study by Abi-Dargham *et al* (2000*a*). [^{11}C] raclopride was prepared as reported in the study by Mawlawi *et al* (2001).

Positron Emission Tomography Procedures

Fasted animals were initially immobilized with ketamine (10 mg/kg intramuscularly). Anesthesia during preparation and scans was maintained with 2% isoflurane through an endotracheal tube. An intravenous catheter was inserted for radioligand administration, drug administration, and hydration. An arterial catheter was placed in a femoral artery for arterial blood sampling and continuous blood pressure monitoring. Vital signs (blood pressure, pulse, electrocardiograph, temperature, and respiration) were monitored continuously using a patient monitoring system (DataScope Corp, Paramus, NJ, USA). Temperature was maintained at 37°C with a heated water blanket. All scanning was performed on an HR+ scanner (Siemens, Knoxville, TN, USA), operating in a three-dimensional mode. The animal's head was placed in the center of the field of view. A 10-minute transmission scan was acquired before tracer injection for attenuation correction. Radioligands were administered as a 30-second intravenous bolus. Emission data were binned into a sequence of frames of increasing length. Total scan durations were 90 minutes for [^{11}C] NNC112 and 60 minutes for [^{11}C] raclopride. On each study day, two scans were acquired: a baseline scan, followed by a second scan during DAR-0100A infusion as described above. Positron emission tomography data were corrected for attenuation, scatter, and randoms and reconstructed using filtered back-projection with a Shepp filter (cutoff 0.5 cycles per projection ray).

Arterial plasma samples were collected using an automated sampling system during the first 4 minutes (11 samples), and manually thereafter at longer intervals. A total of 21 ([^{11}C] NNC112) or 20 ([^{11}C] raclopride) arterial

samples were collected for input function measurement. Five additional samples were collected during each scan for high-performance liquid chromatography analysis of the unmetabolized fraction of radiotracer. During the DAR-0100A condition, five additional samples were collected (at 2, 4, 8, 16, and 60 minutes after injection for [^{11}C] NNC112 and at 2, 4,12, 20, and 40 minutes after injection for [^{11}C] raclopride) for high-performance liquid chromatography analysis of the plasma concentration of DAR-0100A.

Data Analysis

Plasma data: Arterial plasma input functions were formed as described previously (Abi-Dargham *et al*, 2000*a*). Briefly, centrifugation was performed to separate the plasma from whole blood, and the activity in plasma was counted on a gamma counter (Wallac 1480, Perkin-Elmer, Boston, MA, USA). The unmetabolized fraction of the radioligand was measured in the five samples collected for this analysis by high-performance liquid chromatography using a fraction collection method. A C-18 Phenomenex analytical column (Phemomenex, Torrence, CA, USA) was eluted with a solvent mixture of 35% acetonitrile and 65% 0.1 mol/L ammonium formate at a flow rate of 2 mL/min for both radiotracers. The eluate was collected in 5 equal-duration fractions over 10 minutes. Parent fraction was computed as the ratio of the activity in fractions 4 and 5 to the sum of activity from all fractions. The peak retention time for the unmetabolized radioligand was 7 minutes and all labeled metabolites eluted earlier than the parent. The measured fractions were fitted to a Hill equation:

$$\text{unmetabolized fraction} = 1 - \frac{at^b}{t^b + c} \qquad (1)$$

with fitted parameters a, b, and c.

Whole-blood activity was multiplied by this parent-fraction curve to obtain an empirical estimate of the unmetabolized radiotracer concentration in arterial plasma. The empirical curve was fitted to a sum of three exponentials starting at the time of peak concentration. This modeled curve was used as the input function for compartment analysis. Peripheral clearance of radiotracer (L/h) was computed as the injected activity divided by the area under the curve of the input function. In addition, three aliquots of arterial plasma collected before radiotracer injection were spiked with radiotracer, and f_p, the fraction of unmetabolized radiotracer that was not bound to plasma proteins, was determined by an ultrafiltration method.

Positron emission tomography data: Decay-corrected reconstructed data were coregistered to T1-weighted anatomic magnetic resonance images acquired for each animal, using maximization of mutual information as implemented in the SPM2 software environment (Friston *et al*, 1995). Regions of interest, ROIs, were drawn on the magnetic resonance images and transferred to the coregistered PET images. Regions of interest included the cortical regions for [^{11}C] NNC112 scans (cingulate, frontal, parietal, temporal, and occipital cortices), as well as the striatum and cerebellum as a reference region for both radioligands. Time–activity curves were generated from the mean activity in each region and each frame. Data were fitted to two models: a two-tissue compartment model (2TC) with arterial plasma input, and with the simplified reference tissue method (SRTM, Lammertsma and Hume, 1996) with the cerebellum as the reference region. The two methods are complementary, as they use partially independent measurements (one uses arterial plasma data and one exclusively brain data) so that the agreement between methods would provide more confidence in results. For 2TC modeling, total distribution volume (V_T) was computed in each region including the cerebellum, and BP_{ND}, the binding potential relative to the nondisplaceable compartment (Innis *et al*, 2007) was computed as

$$\frac{V_T(\text{ROI})}{V_T(\text{CER})} - 1 \qquad (2)$$

BP_{ND} is a directly estimated parameter in the SRTM model. Receptor occupancy by DAR-0100A was estimated as $-\Delta BP_{ND}$, where ΔBP_{ND} is the percentage change in BP_{ND} across conditions,

$$\Delta BP_{ND} = \frac{BP_{ND}(\text{DAR-0100A scan})}{BP_{ND}(\text{Baseline scan})} - 1 \qquad (3)$$

Cortical values were averaged for all subsequent analyses.

DAR-0100A Plasma Concentration and Free Fraction Analyses

Plasma DAR-0100A was determined using liquid chromatography/mass spectrometry with the addition of 2-methyldihydrexidine as the internal standard. After a liquid–liquid extraction with methyl-*tert*-butyl ether from plasma samples buffered at pH 7, the ether was evaporated to dryness and the residue reconstituted with mobile phase. An aliquot of the extract was injected on a Supelco Discovery HS-F5 column (Supelco Inc, Bellefonte, PA, USA) and eluted with 0.02 mol/L ammonium formate:acetonitrile:methanol (60:20:20, ammonium formate pH = 4.0) at a flow rate of 0.85 mL/min. Both compounds were monitored at their respective molecular ions (m/z 268.3 + for DHX and m/z 282.5 + for 2-methyldihydrexidine), using an Agilent Series 1100 MSD (Agilent Technologies Inc, Santa Clara, CA, USA) operating in a positive atmospheric pressure chemical ionization (APCI) selected ion monitoring (SIM) mode. A seven-point calibration curve from 200 to 1 ng/mL of DAR-0100A indicated good linearity with a run time of 10 minutes per injection. Interassay variation based on three sets of quality controls included with each set of samples did not exceed 15.0, 10.3, and 11.3% for low (2 ng/mL), medium (30 ng/mL), and high (75 ng/mL) quality controls, respectively ($n = 6$ days).

The fraction of DAR-0100A in arterial plasma not bound to protein (free fraction) was assessed *in vitro* using ultrafiltration. Blood was collected from three drug-free baboons using EDTA blood collection tubes, and the plasma separated and stored frozen at −20°C. Human plasma was collected from three volunteer subjects and stored similarly. Plasma samples from each species were pooled, and five 0.5 mL aliquots were fortified with 30 μg of

DAR-0100A and 2-mercaptoethanol as an antioxidant. After a 2-hour incubation at 37°C, plasma samples were transferred into centrifugal micropartition tubes (Centrifree, Millipore, Corrigtwohill, Co., Cork, Ireland) and centrifuged at 2,000 r.p.m. for 15 minutes, and a DAR-0100A calibration curve in saline was included for quantification purposes. The ultrafiltrate (20 μL) was injected into the liquid chromatography/mass spectrometry using the same parameters as described above.

Concentration–Occupancy Relationship

The relationship between arterial plasma levels of DAR-0100A and D1 receptor occupancy was fitted to the model

$$\text{Occupancy} = \frac{\text{Occ}_{\text{MAX}} \times C_{\text{DAR-0100A}}}{\text{EC}_{50} + \text{C}_{\text{DAR-0100A}}} \quad (4)$$

where Occ_{MAX} is the modeled maximally obtainable occupancy, $C_{\text{DAR-0100A}}$ the measured average plasma concentration of DAR-0100A (ng/mL), and EC_{50} the modeled plasma concentration associated with 50% receptor occupancy. The model was fitted semi-logarithmically (occupancy versus $\log_{10} C_{\text{DAR-0100A}}$) using a combination of Prism software (GraphPad Software, Inc, La Jolla, CA, USA) and in-house programs written in Matlab (The Mathworks Inc, Natick, MA, USA). Several models were tested, including a four-parameter model (Occ_{MAX} and EC_{50} the in cortex and striatum separately), a three-parameter model (Occ_{MAX} for the cortex and striatum and global EC_{50}), a one-parameter model in the striatum only (EC_{50} estimated with Occ_{MAX} constrained to 100%), and a one-parameter model in the striatum and cortex (global EC_{50} in the striatum and cortex, Occ_{MAX} in the striatum constrained to 100%, and Occ_{MAX} in the cortex constrained to the value of the ratio $\Delta\text{BP}_{\text{ND}}$(cortex)/$\Delta\text{BP}_{\text{ND}}$(striatum), see below). Cortical Occ_{MAX} for the models in which this parameter was estimated (not fixed) was interpreted as the maximal percentage decrease of [^{11}C] NNC112 binding, and not as the percentage of D1 receptors occupied, as we knew *a priori* that DAR-0100A would not compete with [^{11}C] NNC112 binding at 5-$\text{HT}_{2\text{A}}$ receptors. The constraint formula

$$\text{OCC}_{\text{MAX}}(\text{cortex}) = \frac{\Delta\text{BP}_{\text{ND}}(\text{cortex})}{\Delta\text{BP}_{\text{ND}}(\text{striatum})} \quad (5)$$

follows from the assumption that 100% of striatal [^{11}C] NNC112 binding is vulnerable to competition from DAR-100A, whereas only the D1 fraction of cortical [^{11}C] NNC112 binding is vulnerable to competition. (This model does not incorporate multiple affinity states of the D1 receptors for agonist binding or other mechanisms that may lead to regionally different affinities; see the 'Discussion' section.) Under these circumstances, baseline [^{11}C] NNC112 BP_{ND} in the cortex is

$$f_{\text{ND}}\left(\frac{B_{\text{AVAIL}}(D_1)}{K_{\text{D}}(D_1)} + \frac{B_{\text{AVAIL}}(5\text{-HT}_{2\text{A}})}{K_{\text{D}}(5\text{-HT}_{2\text{A}})}\right) = \text{BP}_{\text{ND}}(D_1) + \text{BP}_{\text{ND}}(5\text{-HT}_{2\text{A}}) \quad (6)$$

where B_{AVAIL}(R) refers to the receptor availability of receptor type R and K_{D}(R) refers to the dissociation constant of [^{11}C] NNC112 for receptor type R. The DAR-0100A condition BP_{ND} is

$$f_{\text{ND}}\left(\frac{B_{\text{AVAIL}}(D_1)}{K_{\text{D}}(D_1)\left(1 + \frac{\text{Free}_{\text{DAR-0100A}}}{\text{Ki}_{\text{DAR-0100A}}}\right)} + \frac{B_{\text{AVAIL}}(5\text{-HT}_{2\text{A}})}{K_{\text{D}}(5\text{-HT}_{2\text{A}})}\right) \quad (7)$$

where $\text{Free}_{\text{DAR-0100A}}$ and $\text{Ki}_{\text{DAR-0100A}}$ are the concentration and inhibition constants of DAR-0100A, respectively, and the percentage change is therefore

$$\text{occupancy} \times \frac{\text{BP}_{\text{ND}}(D_1)}{\text{BP}_{\text{ND}}(\text{total})} \quad (8)$$

whereas in the striatum, $\Delta\text{BP}_{\text{ND}}$ is a direct estimate of D1 occupancy, so that the ratio of ΔBP between regions is an estimate of the fraction of cortical [^{11}C] NNC112 BP_{ND} attributable to D1 binding. Under the assumption that DAR-0100A can occupy 100% of D1 receptors but no 5-$\text{HT}_{2\text{A}}$ receptors, this quantity is the maximal possible decrease, i.e., OCC_{MAX} in the cortex. The models that used all 12 data points ($\Delta\text{BP}_{\text{ND}}$ in the cortex and striatum) and the same analysis method (either 2TC or SRTM) were compared for goodness of fit using the small-sample Akaike information criterion (Burnham and Anderson, 1998).

Results

Effects of DAR-0100A

Blood pressure decreased during administration of DAR-0100A (Figure 1). There was an initial dose-dependent sharp decrease at the beginning of DAR-0100A infusion that tended to rebound to a stable value of ~80% of baseline for the remainder of the infusion without the need for pharmacological intervention.

DAR-0100A Plasma Concentrations and Free Fractions

DAR-0100A plasma concentrations were well identified in liquid chromatography/mass spectrometry chromatograms. DAR-0100A eluted at 4.56 minutes, whereas 2-methyldihydrexidine eluted at 6.40 minutes. Two additional peaks at 7.74 and 8.28 minutes were seen and were most likely *in vivo* metabolic by-products of DAR-0100A (Supplementary Figure). Measured plasma levels of DAR-0100A ranged from 17 to 314 ng/mL in [^{11}C] NNC112 experiments and were 152 ± 219 ng/mL in [^{11}C] raclopride experiments. Plasma concentrations varied monotonically with injected doses, except for one 3 mg/kg dose in which the concentration was lower than expected (Figure 2). The mean free fraction of DAR-0100A in arterial plasma was 0.46% ± 0.14% in baboons and 0.16% ± 0.05% in humans ($P = 0.002$, two-group t-test).

D1 Receptor Binding

[^{11}C] NNC112 scan parameters (parameters not directly associated with specific binding) are presented in Table 1. There were no statistically significant differences in any of these between

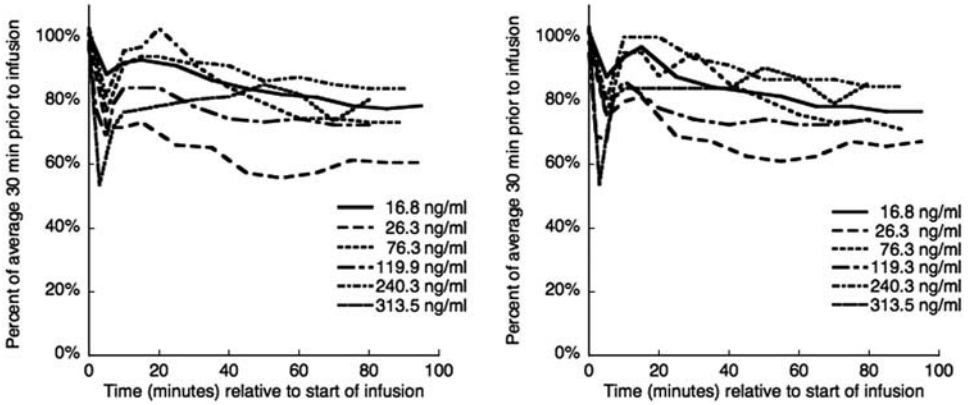

Figure 1 Systolic (left) and diastolic (right) blood pressure during [^{11}C] NNC112 scans with DAR-0100A infusion. In each case, there was a rapid decrease at the start of the infusion, followed (in five of six cases) by a rebound to ~80% of the baseline value without the need for pharmacological intervention.

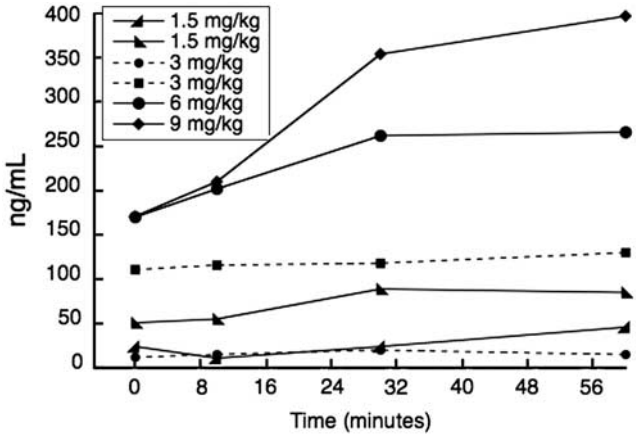

Figure 2 Arterial plasma concentration (ng/mL) of DAR-0100A as a function of time. Plasma concentrations were monotonically related to injected doses in mg/kg, except for one 3 mg/kg dose (– – ● – –) for which plasma concentrations were lower than expected.

baseline and the DAR-0100A condition. However, there was a significant increase in the rate of metabolism of [^{11}C] NNC112 in arterial plasma during the DAR-0100A condition ($P = 0.004$, linear mixed model). There was no significant DAR-0100A dose dependency of this effect; metabolism increased by similar amounts after all doses of DAR-0100A (Figure 3). BP_{ND} values are presented in Table 2, along with the average plasma concentrations of DAR-0100A for each scan. A clear concentration–occupancy relationship was observed in the striatum using both methods of analysis (Table 2, Figure 4). With both methods, apparent occupancy in the cortex was lower than in the striatum. The ratio of cortical to striatal occupancy across studies with the four highest plasma concentrations of DAR-0100A were 36% ± 15% for 2TC and 51% ± 6% for SRTM; these were the values entered into the 'ratio constraint' occupancy model. It is noteworthy that both values (36 and 51%) were lower than the 65% to 70% values predicted by equation (8) based on previous imaging studies with [^{11}C] NNC112. The estimated EC_{50} and maximal D1 receptor occupancy are shown in Table 3.

D2 Receptor Binding

[^{11}C] raclopride scan parameters are presented in Table 1. There were no significant differences in any scan parameter across conditions. The average plasma concentration of DAR-0100A across the three studies was 152 ± 212 ng/mL (range: 16 to 395 ng/mL). This range was unexpectedly wide, given the concentrations observed in the [^{11}C] NNC112 scans after comparable doses. We do not know the cause for this, but in the absence of evidence of experimental or measurement error, we included all data for completeness. In contrast to [^{11}C] NNC112, DAR-0100A had only a small effect on the rate of metabolism of [^{11}C] raclopride in arterial plasma that reached the trend level ($P = 0.07$), as unmetabolized radioligand was only reduced several percentage compared with baseline (Figure 3). There was no detectable effect of DAR-0100A on [^{11}C] raclopride binding in the striatum (2TC $BP_{ND} = 3.43 \pm 0.31$ at baseline and 2TC $BP_{ND} = 3.47 \pm 0.18$ following DAR-0100A, $P = 0.77$, SRTM $BP_{ND} = 2.76 \pm 0.23$ at baseline and SRTM $BP_{ND} = 2.77 \pm 0.17$ following DAR-0100A, $P = 0.90$, $n = 3$).

Discussion

The main findings of this study are as follows: (1) A clear concentration–occupancy relationship was observed between DAR-0100A plasma levels and D1 receptor occupancy measured as ΔBP_{ND}, but high concentrations, relative to feasible doses for humans, were necessary to reach detectable levels of occupancy; (2) there was no detectable binding of DAR-

Table 1 Scan parameters

	V_{ND}	f_p	*ID (mCi)*	*IM (μg)*	*SA (Ci/mmol)*	*CL (L/h)*
[11C] NNC 112						
Baseline	5.15 ± 1.15	0.02 ± 0.01	3.26 ± 1.47	0.96 ± 0.21	1242.82 ± 754.41	58.98 ± 36.22
DAR-0100A	5.07 ± 1.24	0.02 ± 0.00	4.09 ± 1.05	0.91 ± 0.22	1589.82 ± 674.79	61.58 ± 22.16
t-Test (*P*)	0.90	0.37	0.27	0.79	0.51	0.91
[11C] raclopride						
Baseline	0.97 ± 0.13	0.13 ± 0.02	2.86 ± 0.76	0.91 ± 0.1	1120.26 ± 408.01	32.86 ± 4.99
DAR-0100A	1.16 ± 0.16	0.14 ± 0.02	2.36 ± 1.11	0.88 ± 0.14	1005.16 ± 651.78	50.34 ± 26.83
t-Test (*P*)	0.15	0.36	0.47	0.29	0.68	0.30

Means and s.d. are based on $n = 6$ baseline and $n = 6$ DAR-0100A scans for [11C] NNC112 and $n = 3$ baseline and $n = 3$ DAR-0100A scans for [11C] raclopride.

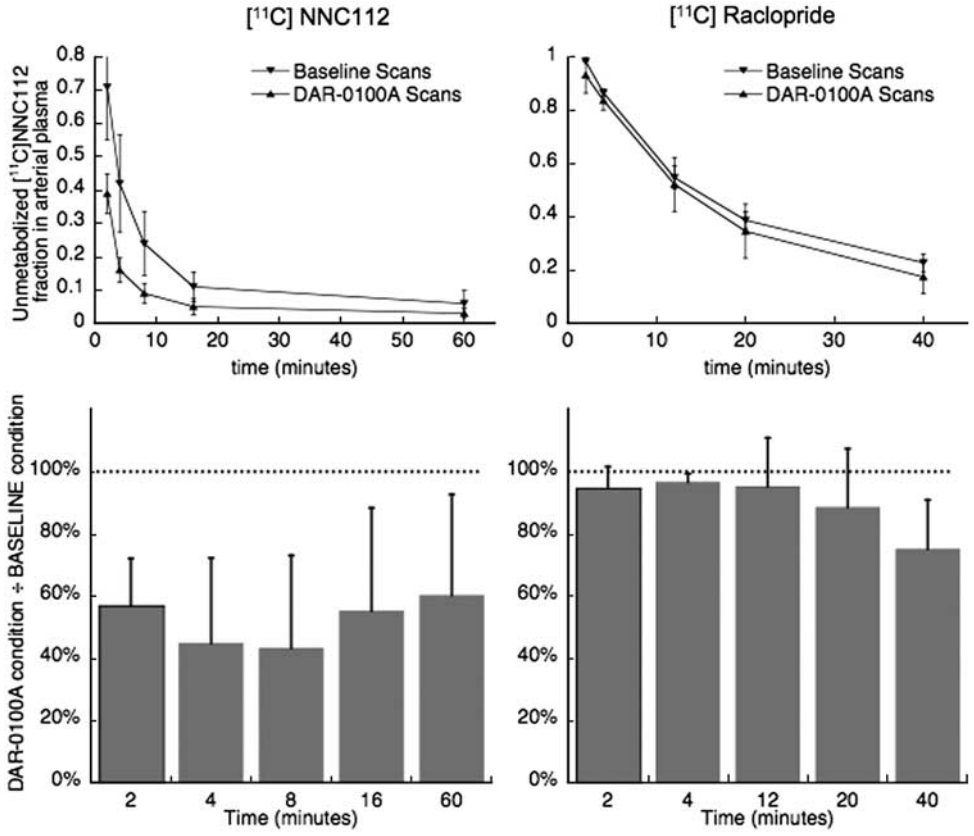

Figure 3 Unmetabolized fraction of radiotracer in arterial plasma as a function of time. DAR-0100A caused a pronounced increase in the rate of metabolism of [11C] NNC112 (left) but only a slight increase for [11C] raclopride (right). Top: markers (▼ = baseline, ▲ = DAR-0100A condition) and error bars are mean ± s.d. across $n = 6$ baseline and $n = 6$ DAR-0100A scans for [11C] NNC112 and $n = 3$ baseline and $n = 3$ DAR-0100A scans for [11C] raclopride. Continuous curves are for visual display only and do not represent statistically modeled fits. Bottom: unmetabolized fraction of radioligand during DAR-0100A condition as a percentage of the fraction during the baseline scan.

0100A to D2 receptors at similarly high concentrations; (3) without the application of a constraint to the concentration–occupancy relationship, the estimated maximal occupancy was <100% and the EC_{50} estimates covered a large range (154 to 547 ng/mL, Table 3) depending on which model was used, suggesting a 'ceiling effect' of <100% occupancy of D1 receptors; and (4) finally, although we did expect, *a priori*, that ΔBP_{ND} would be less in the cortex than in the striatum owing to 5-HT_{2A} binding by [11C] NNC112, the magnitude of the difference was larger than expected. We discuss these findings below, starting with the first two that are most relevant to the design of trials with DAR-0100A in patients.

(1) D1 Occupancy

Tables 2 and 3 and Figure 4, especially results in the striatum, show clearly that D1 occupancy was an

Table 2 [^{11}C] NNC 112 BP_{ND}

	Average of cortical regions			*Striatum*		
ng/mL	*Baseline*	*DAR-0100A*	*ΔBP (%)*	*Baseline*	*DAR-0100A*	*ΔBP (%)*
2TC						
16.83	1.18 ± 0.12	1.27 ± 0.11	8.2 ± 2.7	6.37	6	−5.7
26.25	1.18 ± 0.16	1.39 ± 0.16	18.6 ± 4	5.33	6.08	14.1
76.33	1.14 ± 0.2	1.01 ± 0.16	−11.6 ± 2	5.73	4.54	−20.9
119.92	1.02 ± 0.2	0.96 ± 0.14	−5.6 ± 8.5	5.88	4.21	−28.3
240.33	1.21 ± 0.22	1.09 ± 0.18	−9.5 ± 6.7	6.18	4.5	−27.1
313.5	1.08 ± 0.1	0.96 ± 0.09	−10.8 ± 1.7	5.51	3.64	−33.9
SRTM						
16.83	1.16 ± 0.11	1.13 ± 0.09	−2.9 ± 1.6	4.99	4.94	−1
26.25	1.09 ± 0.14	1.14 ± 0.13	5.2 ± 3	4.63	4.65	0.6
76.33	0.98 ± 0.17	0.87 ± 0.14	−10.6 ± 1.9	4.96	3.99	−19.4
119.92	0.91 ± 0.18	0.74 ± 0.11	−17.5 ± 7.4	4.81	3.28	−31.7
240.33	1.05 ± 0.19	0.91 ± 0.14	−13 ± 3.6	5.1	3.55	−30.5
313.5	1 ± 0.1	0.81 ± 0.06	−18.4 ± 3.1	4.85	3.15	−35

SRTM, simplified reference tissue method; 2TC, two-tissue compartment.
Cortical values are the mean ± s.d. across $n = 5$ cortical regions for each scan.

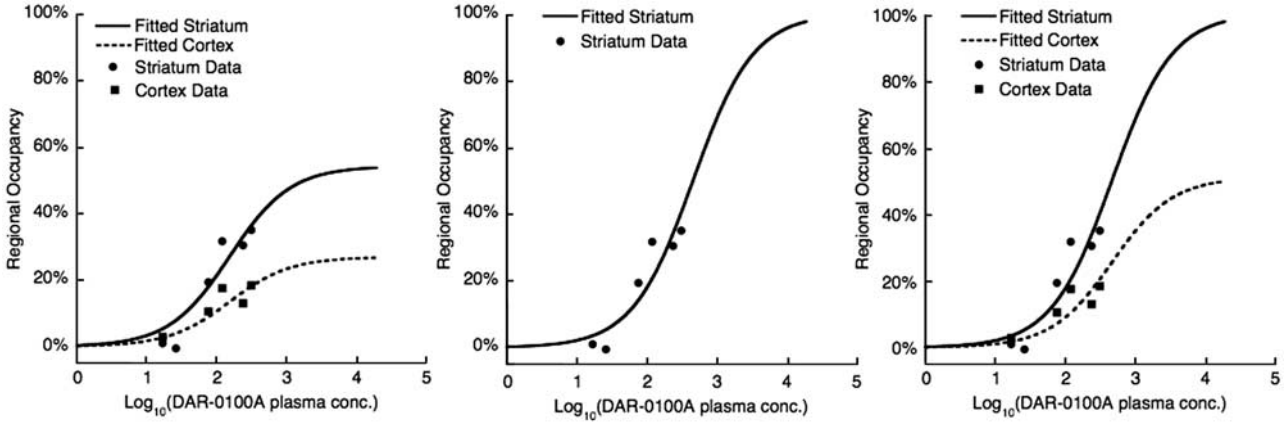

Figure 4 Data fits of the concentration–occupancy relationship between average arterial plasma concentration of DAR-0100A and [^{11}C] NNC112 ΔBP_{ND} measured with PET. Data are from all six [^{11}C] NNC112 studies (two subjects, each at three different DAR-0100A doses). Left panel: fitted parameters were maximal occupancy (each region) and EC_{50} (global). Center panel: EC_{50} fitted in the striatum only with maximal occupancy constrained to 100%. Right panel: EC_{50} fitted globally with maximal occupancy constrained to 100% in the striatum and the average ratio of the striatum to cortical occupancy in the cortex. See the section 'Materials and methods' for derivation and Table 3 for estimated parameters. PET, positron emission tomography.

increasing function of DAR-0100A plasma concentration. To our knowledge, this is the first demonstration *in vivo* of the vulnerability of a D1 radioligand to a D1 agonist compound. Previous tests of vulnerability to fluctuations in the levels of endogenous dopamine using the closely related radioligand [^{11}C] NNC756 were negative (Abi-Dargham *et al*, 1999). This is in contrast with D2 radioligands, many of which have been used to detect dopamine fluctuations after challenges, such as amphetamine or the dopamine transporter blocker methylphenidate (for review, see Laruelle, 2000).

However, plasma concentrations required to reach detectable D1 occupancy were high, and likely to be much higher than those in humans, based on the doses administered to humans to date (George *et al*, 2007). Low occupancy may be related, in part, to the small plasma free fraction of DAR-0100A measured in this study (<1%). Free fractions this low are difficult to measure with high precision, but the measurements were of similar order of magnitude in humans and baboons, suggesting that low free fraction would have a similar effect on the concentration–occupancy relationship in both species. Recently, we administered 10 mg infusions of DAR-0100A to two human subjects and observed DAR-0100A plasma concentration of 1.4 ± 0.5 ng/mL (AA, unpublished data). The free fraction of DAR-0100A in human arterial plasma, based on our data, is 3/8 as large as that in baboon arterial plasma. On the basis of EC_{50} and OCC_{MAX} estimates in Table 3, and assuming similar blood–brain barrier permeability,

Table 3 Occupancy model estimates

Constraint	*Method*	*Regions*	*Cort EC_{50}*	*STR EC_{50}*	*Cort OCC_{MAX} (%)*	*STR OCC_{MAX} (%)*	*AICC*	*10 mg occ. in humans (%)*
No constraint	2TC	Both	DNC	214.0	DNC	53.83	[a]32.16	0.13
Global EC_{50}	2TC	Both	259.6	259.6	18.3	63.9	62.98	0.13
No constraint	SRTM	Both	160.9	154.1	27.37	54.09	52.14	0.18
Global EC_{50}	SRTM	Both	154.7	154.7	26.9	54.18	47.43	0.18
Str 100%	2TC	STR		530.2		100	30.18	0.10
Str 100%	SRTM	STR		464.7		100	25.02	0.11
Ratio constraint	2TC	Both		546.5	31	100	56.64	0.10
Ratio constraint	SRTM	Both		471.1	51	100	44.00	0.11

AICC, Akaike information criterion; Cort, cortex; DNC, did not converge; SRTM, simplified reference tissue method; STR, striatum; 2TC, two-tissue compartment.
All concentrations are in ng/mL.
[a]AICC for the 2TC unconstrained model is for the striatum only owing to the nonconvergence in the cortex; i.e., it is directly comparable only with the 2TC striatum fit with $OCC_{MAX} = 100\%$ constraint. AICC is displayed in 'less is better' form, and direct comparisons are only valid for models using the same data. Human occupancy estimates (column 9) represent the estimated fraction of all D1 receptors bound by DAR-0100A after a 10 mg infusion. These were derived by application of equation (4), using the observed arterial plasma concentration measured in $n = 2$ human subjects who received 10 mg infusions of DAR-0100A, the EC_{50} and maximal occupancy estimates in the striatum (columns 5 and 7) and the ratio of plasma free fraction of DAR-0100A in humans to that in baboons (3/8).

this plasma level would lead to D1 occupancy in the range of 0.1% to 0.2%. Thus, all models predict a very small fraction of D1 receptor occupancy with human dosing. At present, the level of D1 receptor occupancy by DAR-0100A necessary for cognitive improvements is not known. However, there is some indication from preclinical studies that, at least with some D1 agonists, the necessary occupancy level may be extremely low. Castner *et al* (2000) administered very small quantities (10^{-5} to 10^{-4} mg/kg intramuscularly) of the D1 agonist ABT 431 subchronically to monkeys with chronic haloperidol-induced spatial working memory deficits, and detected quantifiable, long-lasting improvements. The appropriate level of receptor binding necessary for a given level of response is a function of the interaction between receptor and ligand and could vary across ligands (Kenakin, 1986; Weiss *et al*, 1996*a*); therefore, a direct measurement of cognitive effects will be necessary to determine whether there is a DAR-0100A dose that leads to detectable cognitive improvement in patients with schizophrenia. However, given that test–retest reproducibility of human striatal [^{11}C] NNC112 BP_P and BP_{ND} are both $\sim$15% (Abi-Dargham *et al*, 2000*b*), PET imaging of DAR-0100A receptor occupancy in humans can be expected to yield effect sizes on the order of 0.01, which cannot be reliably measured.

(2) D2 Occupancy

In this study, [^{11}C] raclopride binding was unaffected by very high doses of DAR-0100A. The mean plasma concentration of DAR-0100A during [^{11}C] raclopride scans was 152 ng/mL, which is 100-fold greater than that observed in humans receiving 10 mg of DAR-0100A. At this concentration, models in Table 3 predict D1 receptor occupancy to be between 24 and 37%. Thus, it can be expected that occupancy of D2 receptors will remain negligible at any dose of DAR-0100A administered to humans, and that even if doses that attain sizable D1 occupancy can be achieved safely, they will still lead to virtually no D2 occupancy.

(3) Ceiling Effects and the Choice of Occupancy Model

The estimates of the pharmacokinetic parameter EC_{50} varied considerably according to whether the constraint that full occupancy was attainable was invoked. Given the wide range of EC_{50} estimates, it is important to compare the relative accuracy of the various methods. Statistically, models with maximal striatal binding constrained to 100% were more favored by the Akaike information criterion, indicating more parsimonious explanation of the data (Table 3). Maximal occupancy is difficult to estimate accurately in the absence of measurements showing occupancy close to the putative maximum, i.e., in the upper arm of the curves in Figure 4, over a wide range of ligand concentrations. However, it was not possible to increase DAR-0100A concentrations beyond those used in this study because of the peripheral effects on blood pressure. Although a purely statistical interpretation favors full occupancy models, models predicting a ceiling effect are also consistent with the possibility that a fraction of D1 receptors available for [^{11}C] NNC112 binding are not available to DAR-0100A binding at any concentration. A ceiling effect could be related to the following:

Multiple affinity states and ceiling effect: As DAR-0100A is an agonist, there are likely to be multiple conformations of the receptor, some of which bind DAR-0100A with higher affinity than others. However, interconvertible affinity states alone should not limit access to these receptors at high enough

DAR-0100A concentrations, and in this situation, DAR-0100A occupancy is likely to follow a one-site fit. The cubic ternary complex model provides a thermodynamically comprehensive description of the equilibrium binding of agonists to G protein-coupled receptors having multiple conformations (Weiss *et al*, 1996*b*). According to the cubic ternary complex model, the fractional occupancy of receptors by an agonist will follow a one-site fit with an apparent association constant (reciprocal of the apparent dissociation constant) equal to a weighted sum of the association constants of the agonist for various states of the receptors (active conformation or not, G protein bound or not), with weights given by the equilibrium fraction of the total receptor concentration represented by each state (Weiss *et al*, 1996*c*). When the G protein is in excess such that unbound G protein concentration is approximately constant independent of the level of agonist binding, the weighted association parameter is constant at all levels of the agonist (see Appendix A) and will tend to favor the affinity for the state that is more prevalent in the native system. When G protein availability is rate limiting, the apparent association constant can be different at each level of agonist, with the balance shifting toward the affinity for the inactive conformation (Appendix A), but because the apparent affinity shifts continuously as a function of DAR-0100A concentration, the resulting curves will be difficult to distinguish from a one-site model (Appendix A). Still, we cannot rule out the possibility that agonist binding has a low affinity component that is not rapidly interconverting and that this leads to a component of antagonist binding that cannot be inhibited without going to much higher concentrations of the agonist.

There is considerable evidence that many G protein-coupled receptors form dimers and oligomers (Lee *et al*, 2003; Milligan, 2004), including D1 receptors (Kong *et al*, 2006; Fiorentini *et al*, 2008). Results consistent with negative cooperativity between agonist (but not antagonist) binding to two protomers in a dimer have been reported (Kara *et al*, 2010). Such a scenario might also potentially lead to a relative inability of agonist to occupy the second protomer in a dimer, which might also lead to difficulty in inhibiting all antagonist binding.

Receptor internalization and ceiling effect: It is well documented that agonist binding induces D1 receptors' internalization (Dumartin *et al*, 1998), and this effect has been shown in cell preparations with dihydrexidine (Ryman-Rasmussen *et al*, 2005). To cause a ceiling effect, this scenario would require that internalized receptors be available for [^{11}C] NNC112 binding, but not for DAR-0100A binding. To our knowledge, this effect has not been studied in the setting of D1 receptors and DAR-0100A. A recent study examined internalization of D2 receptors and binding of D2 selective ligands (Guo *et al*, 2010). Five of the six antagonists tested bound to the internalized D2 receptor with relatively small alterations in affinity, whereas the charged hydrophilic antagonist sulpiride and the agonist dopamine had greatly reduced affinity for internalized receptors, consistent with their more limited penetration of the plasma membrane. Although this study was performed in a different receptor system (D2 versus D1), to the degree it can inform the current study, it suggests that many ligands are capable of binding to internalized receptors, and that both DAR-0100A and [^{11}C] NNC112 might readily bind to internalized receptors. The requirement for a ceiling effect would be that the ratio of affinities, $K_{\text{D-DAR-0100A}}/K_{\text{D-NNC112}}$, is greatly increased for internalized receptors relative to surface receptors. In the absence of data about DAR-0100A and [^{11}C] NNC112 binding to internalized receptors, this scenario cannot be ruled out.

In summary, although the full occupancy model is favored on statistical grounds, there are scenarios in which a ceiling effect could occur, and currently, there is insufficient experimental evidence to determine how plausible these are. Nonetheless, regardless of which model is invoked, the predicted D1 occupancy for a 10 mg dose in human would be extremely small.

(4) Differences in Regional Occupancy

Measured ΔBP_{ND} in the cortex was either 35% (2TC) or 51% (SRTM) of measured striatal ΔBP_{ND}. We did expect, *a priori*, that cortical ΔBP_{ND} would be less than striatal ΔBP_{ND} because of the binding of [^{11}C] NNC112 to 5-HT_{2A} receptors. However, the extent of the observed difference was greater than we would have predicted based on this phenomenon alone. The portion of cortical binding attributed to 5-HT_{2A} we have measured previously was in the range of 25% to 35% (Ekelund *et al*, 2007; Slifstein *et al*, 2007), so that according to equation (8), cortical ΔBP_{ND} should have been between 65 and 75% of striatal ΔBP_{ND}. This suggests that additional factors may have led to decreased affinity of DAR-0100A for cortical, versus striatal D1 receptors. One possibility is that the equilibrium fraction of receptors configured in the high-affinity state for agonists is lower in the cortex than in the striatum, so that DAR-0100A competes more effectively with [^{11}C] NNC112 in the striatum than in the cortex. This could be brought about by any factor that would increase the expression for K_{App} in equation (A1) in the striatum compared with that in the cortex, such as increased G-protein concentration or some factor that would increase the equilibrium fraction of receptors in the active state, assuming these have higher affinity for agonists than those in the inactive state as in the cubic ternary complex model (i.e., $\alpha > 1$). It is also conceivable that receptor dimerization or heteromerization might differ across brain regions, and that this could have a role as described above.

Another potential explanation of the observation of lower than expected binding in the cortex is that it is an artifact of the interaction of the radioligand kinetics with the DAR-0100A kinetics. ΔBP_{ND}, or the portion attributable to D1 in this case, can be shown to be a weighted average of the receptor occupancy by drug over the course of the scan with weight at time t (Endres and Carson, 1998; Kegeles *et al*, 2008):

$$w(t) = \frac{C_{ND}(t)}{\int_0^\infty C_{ND}(\tau)d\tau}$$
$$\Delta BP_{ND} = \int_0^\infty w(t) \times \text{Occupancy}(t) dt \quad (9)$$

Because, owing to large differences in receptor concentration, the kinetics of the nondisplaceable component of [^{11}C] NNC112 in the brain (C_{ND}) are different in the cortex and striatum, the weights in equation (9) will tend to be larger in the cortex earlier in the scan compared with the striatum; the weights in the striatum will be more evenly distributed across the whole duration of the scan. If receptor occupancy was increasing over the course of the scan, the net effect would be increased apparent occupancy in the striatum compared with the cortex. Owing to peripheral side effects (Figure 1) it was not possible to give a priming bolus before the constant infusion of DAR-0100A, and therefore it is plausible that D1 receptor occupancy was increasing over the course of the scan.

Conclusions

In this study, the dopamine D1 receptor agonist DAR-0100A was shown to compete effectively with the D1 antagonist radiotracer [^{11}C] NNC112. A clear dose–occupancy relationship was observed, especially in the striatum where [^{11}C] NNC112 specific binding is almost exclusively attributed to D1 receptors. Several models were used to estimate the pharmacokinetic parameters of DAR-0100A, all of which indicated that doses in the range of 10 mg will lead to $<1\%$ receptor occupancy in humans. Binding of DAR-0100A to D2 receptors was undetectable using PET imaging with [^{11}C] raclopride at doses that lead to D1 occupancy in excess of 30%. In conclusion, DAR-0100A in arterial plasma enters the primate brain and binds with specificity to D1 receptors, but high concentrations are required to reach quantifiable levels, such that occupancy will likely be undetectable in humans by *in vivo* imaging methods.

Acknowledgements

We gratefully acknowledge the expert technical contributions of Elizabeth Hackett, John Castrillon, Sung A Bae, and Xiaoyan Xu, PhD.

Conflict of interest

The authors declare no conflict of interest.

References

Abi-Dargham A, Martinez D, Mawlawi O, Simpson N, Hwang DR, Slifstein M, Anjilvel S, Pidcock J, Guo NN, Lombardo I, Mann JJ, Van Heertum R, Foged C, Halldin C, Laruelle M (2000*a*) Measurement of striatal and extrastriatal dopamine D-1 receptor binding potential with [C-11]NNC 112 in humans: validation and reproducibility. *J Cereb Blood Flow Metab* 20:225–43

Abi-Dargham A, Martinez D, Mawlawi O, Simpson N, Hwang DR, Slifstein M, Pidcock J, Guo N, Lombardo I, van Heertum R, Foged C, Halldin C, Mann JJ, Laruelle M (2000*b*) Measurement of striatal and extrastriatal dopamine D1 receptor binding potential with [11C]NNC 112 in humans: validation and reproducibility. *J Cereb Blood Flow Metab* 20:225–43

Abi-Dargham A, Simpson N, Kegeles L, Parsey R, Hwang DR, Anjilvel S, Zea-Ponce Y, Lombardo I, Van Heertum R, Mann JJ, Foged C, Halldin C, Laruelle M (1999) PET studies of binding competition between endogenous dopamine and the D-1 radiotracer [C-11]NNC 756. *Synapse* 32:93–109

Aleman A, Hijman R, de Haan EHF, Kahn RS (1999) Memory impairment in schizophrenia: a meta-analysis. *Am J Psychiatry* 156:1358–66

Arnsten AF, Cai JX, Murphy BL, Goldman-Rakic PS (1994) Dopamine D1 receptor mechanisms in the cognitive performance of young adult and aged monkeys. *Psychopharmacology* 116:143–51

Burnham K, Anderson D (1998) *Model Selection and Inference: A Practical Information Theoretic Approach*. New York: Springer, 353pp

Castner SA, Williams GV, Goldman-Rakic PS (2000) Reversal of antipsychotic-induced working memory deficits by short-term dopamine D1 receptor stimulation. *Science* 287:2020–2

Dumartin B, Caille I, Gonon F, Bloch B (1998) Internalization of D1 dopamine receptor in striatal neurons *in vivo* as evidence of activation by dopamine agonists. *J Neurosci* 18:1650–61

Durstewitz D, Seamans JK (2002) The computational role of dopamine D1 receptors in working memory. *Neural Netw* 15:561–72

Durstewitz D, Seamans JK (2008) The dual-state theory of prefrontal cortex dopamine function with relevance to Catechol-O-Methyltransferase genotypes and schizophrenia. *Biol Psychiatry* 64:739–49

Ekelund J, Slifstein M, Narendran R, Guillin O, Belani H, Guo NN, Hwang Y, Hwang DR, Abi-Dargham A, Laruelle M (2007) *In vivo* DA D-1 receptor selectivity of NNC 112 and SCH 23390. *Mol Imaging Biol* 9:117–25

Endres CJ, Carson RE (1998) Assessment of dynamic neurotransmitter changes with bolus or infusion delivery of neuroreceptor ligands. *J Cereb Blood Flow Metab* 18:1196–210

Fiorentini C, Busi C, Gorruso E, Gotti C, Spano P, Missale C (2008) Reciprocal regulation of dopamine D1 and D3 receptor function and trafficking by heterodimerization. *Mol Pharmacol* 74:59–69

Friston KJ, Holmes AP, Worsley KJ, Poline J-P, Frith CD, Frakowiak RSJ (1995) Statistical parametric maps in

functional imaging: a general linear approach. *Hum Brain Mapp* 2:189–210

George MS, Molnar CE, Grenesko EL, Anderson B, Mu QW, Johnson K, Nahas Z, Knable M, Fernandes P, Juncos J, Huang XM, Nichols DE, Mailman RB (2007) A single 20 mg dose of dihydrexidine (DAR-0100), a full dopamine D-1 agonist, is safe and tolerated in patients with schizophrenia. *Schizophr Res* 93:42–50

Goldman-Rakic PS, Castner SA, Svensson TH, Siever LJ, Williams GV (2004) Targeting the dopamine D-1 receptor in schizophrenia: insights for cognitive dysfunction. *Psychopharmacology* 174:3–16

Guo N, Guo W, Jiang M, Schieren I, Narendran R, Slifstein M, Abi-Dargham A, Javitch J, Laruelle M, Rayport S (2010) Impact of D2 receptor internalization on binding affinity of positron emission tomography radiotracers. *Neuropsychopharmacology* 35:806–17

Innis RB, Cunningham VJ, Delforge J, Fujita M, Giedde A, Gunn RN, Holden J, Houle S, Huang SC, Ichise M, Lida H, Ito H, Kimura Y, Koeppe RA, Knudsen GM, Knuuti J, Lammertsma AA, Laruelle M, Logan J, Maguire RP, Mintun MA, Morris ED, Parsey R, Price JC, Slifstein M, Sossi V, Suhara T, Votaw JR, Wong DF, Carson RE (2007) Consensus nomenclature for *in vivo* imaging of reversibly binding radioligands. *J Cereb Blood Flow Metab* 27:1533–9

Kara E, Lin H, Strange P (2010) Co-operativity in agonist binding at the D2 dopamine receptor: evidence from agonist dissociation kinetics. *J Neurochem* 112: 1442–53

Kegeles LS, Slifstein M, Frankle WG, Xu XY, Hackett E, Bae SA, Gonzales R, Kim JH, Alvarez B, Gil R, Laruelle M, Abi-Dargham A (2008) Dose-occupancy study of striatal and extrastriatal dopamine D-2 receptors by aripiprazole in schizophrenia with PET and [F-18] Fallypride. *Neuropsychopharmacology* 33: 3111–3125

Kenakin TP (1986) Receptor reserve as a tissue misnomer. *Trends Pharmacol Sci* 7:93–5

Knoerzer TA, Nichols DE, Brewster WK, Watts VJ, Mottola D, Mailman RB (1994) Dopaminergic benzo[a]-phenanthridines—resolution and pharmacological evaluation of the enantiomers of dihydrexidine, the full efficacy D-1 dopamine-receptor agonist. *J Med Chem* 37:2453–60

Kong MMC, Fan T, Varghese G, O'Dowd BF, George SR (2006) Agonist-induced cell surface trafficking of an intracellularly sequestered D1 dopamine receptor homo-oligomer. *Mol Pharmacol* 70:78–89

Lammertsma AA, Hume SP (1996) Simplified reference tissue model for PET receptor studies. *Neuroimage* 4:153–8

Laruelle M (2000) Imaging synaptic neurotransmission with *in vivo* binding competition techniques: a critical review. *J Cereb Blood Flow Metab* 20:423–51

Lee SP, O'Dowd BF, George SR (2003) Homo- and hetero-oligomerization of G protein-coupled receptors. *Life Sci* 74:173–80

Mawlawi O, Martinez D, Slifstein M, Broft A, Chatterjee R, Hwang DR, Huang YY, Simpson N, Ngo K, Van Heertum R, Laruelle M (2001) Imaging human mesolimbic dopamine transmission with positron emission tomography: I. Accuracy and precision of D-2 receptor parameter measurements in ventral striatum. *J Cereb Blood Flow Metab* 21:1034–57

Milligan G (2004) G protein-coupled receptor dimerization: function and ligand pharmacology. *Mol Pharmacol* 66:1–7

Mottola DM, Brewster WK, Cook LL, Nichols DE, Mailman RB (1992) Dihydrexidine, a novel full efficacy D1-dopamine receptor agonist. *J Pharmacol Exp Ther* 262:383–93

Ryman-Rasmussen JP, Nichols DE, Mailman RB (2005) Differential activation of adenylate cyclase and receptor internalization by novel dopamine D-1 receptor agonists. *Mol Pharmacol* 68:1039–48

Schneider JS, Sun ZQ, Roeltgen DP (1994) Effects of dihydrexidine, a full dopamine D-1 receptor agonist, on delayed-response performance in chronic low-dose MPTP-treated monkeys. *Brain Res* 663:140–4

Seamans JK, Gorelova N, Durstewitz D, Yang CR (2001) Bidirectional dopamine modulation of GABAergic inhibition in prefrontal cortical pyramidal neurons. *J Neurosci* 21:3628–38

Seamans JK, Yang CR (2004) The principal features and mechanisms of dopamine modulation in the prefrontal cortex. *Prog Neurobiol* 74:1–57

Slifstein M, Kegeles LS, Gonzales R, Frankle WG, Xu XY, Laruelle M, Abi-Dargham A (2007) [C-11] NNC 112 selectivity for dopamine D-1 and serotonin 5-HT2A receptors: a PET study in healthy human subjects. *J Cereb Blood Flow Metab* 27:1733–41

Trantham-Davidson H, Neely LC, Lavin A, Seamans JK (2004) Mechanisms underlying differential D1 versus D2 dopamine receptor regulation of inhibition in prefrontal cortex. *J Neurosci* 24:10652–9

Weiss JM, Morgan PH, Lutz MW, Kenakin TP (1996*a*) The cubic ternary complex receptor-occupancy model. 3. Resurrecting efficacy. *J Theor Biol* 181:381–97

Weiss JM, Morgan PH, Lutz MW, Kenakin TP (1996*b*) The cubic ternary complex receptor-occupancy model. 1. Model description. *J Theor Biol* 178:151–67

Weiss JM, Morgan PH, Lutz MW, Kenakin TP (1996*c*) The cubic ternary complex receptor-occupancy model. 2. Understanding apparent affinity. *J Theor Biol* 178:169–82

Appendix A

One of the main results of the cubic ternary complex model (Weiss *et al*, 1996*c*) is the following expression for the apparent association constant of an agonist ligand that binds to a G protein-coupled receptor with multiple affinity states:

$$K_{\mathrm{Aapp}} = \frac{K_{\mathrm{A}}(1 + \alpha K_{\mathrm{ACT}} + \gamma K_{\mathrm{G}}[\mathrm{G}] + \alpha\beta\gamma\delta K_{\mathrm{G}} K_{\mathrm{ACT}}[\mathrm{G}])}{1 + K_{\mathrm{ACT}} + K_{\mathrm{G}}[\mathrm{G}] + \beta K_{\mathrm{G}} K_{\mathrm{ACT}}[\mathrm{G}]} \tag{A1}$$

where [G] is the surface concentration of the unbound G protein and the parameters are defined as follows:

K_{A} Is the association constant (affinity) of the agonist for the inactive conformation of the receptor.

K_{ACT} Is the equilibrium partition between the active and inactive forms of the receptor in the absence of the agonist or G protein.

K_G Is the association constant of the G protein for the inactive conformation of the receptor.

α Is the increase in affinity of the agonist for active compared with inactive conformation of receptor.

β Is the increase in affinity of the G protein for active compared with inactive conformation of receptor.

γ Is the increase in affinity of the agonist for the G protein-bound inactive receptor compared with inactive unbound receptor.

δ Is the synergistic increase in activity of the receptor when both agonist and G protein are bound.

The assumption that all of these lead to increased affinity is equivalent to

$$\alpha, \beta, \gamma, \delta > 1 \tag{A2}$$

From the form of equation (A1), it is apparent that when [G] is large enough such that it is relatively unchanged at different concentrations of agonist, that K_{Aapp} is truly constant, and binding of agonist will follow the apparent one-site curve

$$[AR] = \frac{[A]}{[A] + K_{Aapp}^{-1}} \tag{A3}$$

where [A] is agonist concentration and [AR] the agonist-receptor complex. When [G] is rate limiting, say $[G] < [R_T]$, where $[R_T]$ is the total receptor concentration including all states, K_{Aapp} will be an increasing function of [G], which in turn will be a decreasing function of [A], so that the apparent affinity will shift toward the inactive, i.e., low-affinity state, form. This can be shown mathematically as follows. The apparent association constants for the active and inactive forms of the receptor are, respectively:

$$\begin{aligned} K_{\text{apparent, Active}} &= (\alpha K_A K_{ACT}[R_i] + \alpha\beta\gamma\delta K_A K_G K_{ACT}[R_i][G])/[R_T] \\ K_{\text{apparent, Inactive}} &= (K_A[R_i] + \gamma K_A K_G[R_i][G])/[R_T] \end{aligned} \tag{A4}$$

where $[R_i]$ is the equilibrium concentration of the inactive form. Their ratio is

$$\alpha K_{ACT} \frac{(1 + \beta\gamma\delta K_G[G])}{(1 + \gamma K_G[G])} \tag{A5}$$

which is an increasing function of [G] when $\beta\delta$ is >1, which in turn follows from the assumptions that the G protein favors the active conformation and that there is positive synergy when both the G protein and the agonist are bound to the receptor. As [G] decreases as [A] increases, the weight of the overall apparent association constant can be seen to shift toward the inactive form. This latter fact can be shown analytically ($d[G]/d[A] < 0$ under the stated assumptions) but can also be seen intuitively: as the agonist and the G protein each induce increased affinity of the other for receptor, the more agonist there is bound (the higher [A] is), the more G protein will be bound, and when total G protein is finite, the unbound form [G] will decrease with increasing bound G protein.

Supplementary Information accompanies the paper on the Journal of Cerebral Blood Flow & Metabolism website (http://www.nature.com/jcbfm)